Ultrasonography imaging of the anterolateral ligament using real-time virtual sonography

Title:

Ultrasonography imaging of the anterolateral ligament using real-time virtual sonography

Authors:

Takeshi Oshima[1]

Junsuke Nakase[1]

Hitoaki Numata[1]

Yasushi Takata[1]

Hiroyuki Tsuchiya[1]

Affiliations:

[1]Department of Orthopaedic Surgery, Graduate School of Medical Science, Kanazawa University, 13-1 Takara-machi, Kanazawa 920-8641, Japan

Corresponding author:

Junsuke Nakase, M.D., Ph.D.

Department of Orthopaedic Surgery, Graduate School of Medical Science, Kanazawa University

13-1 Takara-machi, Kanazawa 920-8641, Japan

TEL: +81-76-265-2374

FAX: +81-76-234-4261

E-mail: nakase1007@yahoo.co.jp

Abstract

Background: The anterolateral ligament (ALL) functions as a stabilizer in the internal rotation of the knee.

Previous studies have reported that the ALL can be identified using magnetic resonance imaging (MRI); however, there are no reports on using ultrasonography (US) for this purpose. Real-time virtual sonography (RVS) uses magnetic navigation and computer software for the synchronized display of real-time US and multiplanar reconstruction MRI images. This study investigated the ability and feasibility of using US with RVS to evaluate the ALL.

Methods: Nine healthy subjects were enrolled. All MRI examinations were performed in the coronal plane. The Digital Imaging Communications in Medicine MRI dataset was loaded into the Hitachi Aloka Preirus, and US images were displayed on the same monitor. When the ALL was identified using MRI, the monitor was frozen to evaluate the ALL. The ALL was divided into the femoral, meniscal, and tibial portions. The portions and thickness of the ALLs and the lateral inferior genicular artery (LIGA), a landmark for the ALL, were evaluated.

Results: All portions of the ALL could be identified using MRI. Using US, the tibial portion of the ALL was detected in all subjects and the femoral portion was detected in seven subjects; however, the meniscal portions could not be identified. The average ALL thickness as measured by US was 1.3 ± 0.1 mm and the LIGA was identified in all cases.

Conclusions: Most portions of the ALL can be identified using US. As most ALL injuries occur at the femoral or tibial portion, US may be useful as a diagnostic tool for ALL injury.

Key words: anterolateral ligament; ultrasonography; real-time virtual sonography

Introduction

In 1879, the French surgeon Paul Segond noted that excessive internal rotation of the knee caused a remarkably constant avulsion fracture pattern at the proximolateral tibia [1]. This avulsion fracture, called the Segond fracture, was reported to occur in the tibial region, “definitely posterior and above the tibial tubercle.” At this anatomic location, Segond also demonstrated that excessive internal rotation caused abnormal tension on ‘a pearly, resistant, fibrous band’ attached to the Segond fracture. Despite having been described 130 years ago, this ‘pearly, resistant, fibrous band’ has been poorly investigated.

In 2013, an anatomic study by Claes et al. described this structure as a distinct and consistent structure termed the anterolateral ligament (ALL) of the knee [2]. The ALL is an extra-articular structure with a well-defined course and has been detected in 83% to 100% of individuals [3, 4]. The origin of the ALL is the lateral femoral condyle, which is anterior and distal to the origin of the lateral collateral ligament (LCL) and lies between the LCL and popliteal tendon. The ALL takes an oblique path anteriorly and inferiorly to the tibia, inserting on the lateral meniscus and the lateral tibial condyle, 4.4–11.1 mm below the lateral tibial plateau [2, 5, 6, 7, 8].

Recently, the ALL has become increasingly important [3, 4]. Monaco et al. suggested that it is associated with lesions of the anterior cruciate ligament (ACL) [9] and Parsons et al. noted that the ALL is an important stabilizer of internal rotation at flexion angles > 35° in a cadaveric study [10]. Imaging studies identifying the ALL have also become more important in understanding the anatomy and function of this ligament. Some authors have cited radiological visualization parameters specific to this structure using MRI scans [11, 12, 13]. Helito et al. reported that the ALL could be visualized in 1.5-T MRI scans and could be divided into three portions: the femoral, meniscal, and tibial portions [12].

Ultrasonography (US) is a useful tool for the diagnosis of superficial soft tissue disorders. It allows visualization in any limb position and is noninvasive. The identification of the ALL by US enables comparison with the contralateral side and allows the evaluation of the dynamic motion of the ALL.

Ultimately, US imaging may help clarify the thus far undefined indications for ALL reconstruction. Although a single previous case report presented an ultrasonographic description of the ALL [14], in this report, there was no confirmation that the ultrasonographic images were indeed those of the ALL.

Real-time virtual sonography (RVS) is a new technology that uses magnetic navigation and computer software for the synchronized display of real-time US and multiplanar reconstruction MRI images. Previous studies have reported that the ALL can be identified on MRI [11, 12, 13]. Therefore, in the present study, we use RVS to evaluate the efficacy of ultrasonography in demonstrating the ALL. The purpose of this study was to evaluate the efficacy of ultrasonography in demonstrating the ALL by using real-time virtual sonography (RVS).

Materials and Methods

Nine healthy male volunteers aged 28–37 years old with no history of knee problems were enrolled in this study. The mean age, height, and weight were 30.3 ± 2.6 y, 172.1 ± 3.0 cm, and 71.8 ± 8.7 kg, respectively. An MRI scan of the left knee was performed in each subject subsequently followed by RVS. This study was conducted after receiving approval from the science and research ethics committee at our institution. Written informed consent was obtained from each subject.

MRI protocol

All MRI scans were performed with a 3.0-T MR imager (Signa EXCITE HDx 3.0T, GE Medical Systems, WI, USA) using a dedicated knee coil (quadrature lower extremity coil, Invivo Corporation, USA) with 30° of knee joint flexion. The imaging parameters were as follows: 2,000 ms repetition time (TR), 113.9 ms echo time (TE), 288×288 matrix, 16.0 cm field of view (FOV), 1.0 mm section thickness, ±100.00 kHz bandwidth, echo train length = 10. The coronal view was oriented according to the femur position, parallel to the femoral condyles.

RVS protocol

The fusion imaging system (Real-time Virtual Sonography, HI VISION Preirus, Hitachi Aloka Medical, Japan) was composed of a position-sensing unit mounted on the US unit, a magnetic field transmitter, and a sensor fixed to the probe using a specific bracket (Fig. 1). The magnetic tracking system determined the position and movement of the moveable sensor fixed to the probe during scanning within a defined operating volume. Displacement of the probe remained within 20–70 cm of the magnetic field transmitter. Orientation and position data were transmitted to the US system for computation with the MRI data. The Digital Imaging Communications in Medicine MRI dataset was loaded into the fusion system and displayed together with the US image on the same monitor (RVS imaging; Fig. 2). MRI and US images were then synchronized and manually registered. Registration was performed in the plane in which the popliteal fossa and entire LCL could be visualized at the same time with 30° flexion of the knee joint.

RVS analysis

Two orthopedists (T.O. and H.N.) with experience in musculoskeletal ultrasonographic imaging performed RVS. The orthopedists were familiar with the ALL having previously attended anatomical dissections of the ALL.

The ligament was divided into three portions based on previous anatomical studies [12]: the femoral portion (origin of lateral condyle to the bifurcation point), the meniscal portion (bifurcation to the lateral meniscal insertion), and the tibial portion (bifurcation to the tibial insertion; Fig. 3). Both examiners were able to visualize all portions, including the origin and insertion of the ALL in multiplanar reconstruction MRI images of the RVS in all knees. When the ALL was demonstrated on MRI imaging, the RVS image was frozen and the specifics of the ALL were evaluated using the US images (Figs. 4 and 5). Structures noted on MRI images were confirmed on the US images. The lateral inferior genicular artery (LIGA) was easily visualized using Doppler US imaging. The ALL runs above the LIGA and below the iliotibial band (ITB) and the examiners were able to confirm that the structure attached to the tibia and running between these two landmarks was the ALL. The detection of the ALL portions and the LIGA with US was investigated. The thickness of the ALL above the LIGA, the length of the ALL, and the distance from the tibial insertion to the lateral tibial plateau in the US images were also investigated.

To evaluate interobserver reliability, the intraclass correlation coefficient (ICC) was evaluated. The level of statistical significance was set at $P<0.05$. Statistical analyses were performed using the Statistical Package for the Social Sciences (SPSS) for Windows Version 19.0 (SPSS Inc.; Chicago, IL, USA).

Results

With US imaging, each examiner was able to visualize the femoral and tibial portions of the ALL in all knees. However, the origin of the femoral portion could not be identified with US in two subjects by one observer and in three subjects by the second observer. The insertion of the tibial portion could be identified in all knees (Table 1). On the other hand, the meniscal portion was not visualized in any subject. The results of both observers were averaged. In US the thickness of the ALL above the LIGA was 1.3 ± 0.1 mm, the length of the ALL was 30.4 ± 3.1 mm, and the distance from the tibial insertion to the lateral tibial plateau was 7.9 ± 1.1 mm. In MRI imaging, the thickness of the ALL above the LIGA was 1.1 ± 0.1 mm, the length of the ALL was 31.5 ± 2.2 mm, and the distance from the tibial insertion to the lateral tibial plateau was 7.7 ± 0.6 mm. The results of each observer and the ICC are presented in Table 2.

When the ALL insertion could be identified, the distal edge of the US probe was 20.0 ± 2.4 mm from the fibular head and 22.8 ± 2.5 mm from the Gerdy tubercle. In other words, the tibial insertion was approximately halfway between the midpoint of the fibular head and the Gerdy tubercle.

Discussion

With increasing attention on the ALL, optimal imaging of the ALL has become more important. The key finding of this study is that the ALL could be visualize by US. To our knowledge, this is the first report to investigate the detailed imaging of the ALL with US. RVS has previously been used in the identification and biopsy of breast cancers and abdominal tumors [15, 16, 17, 18, 19]. These studies suggest that the RVS system can accurately identify these tumors. Nakano et al. reported that of 63 breast lesions, 42 (67%) lesions were identified by conventional US, whereas all lesions were identified by RVS [18]. Kitada et al. reported that RVS-guided radiofrequency ablation therapy for hepatocellular carcinomas could be useful for treating hepatocellular carcinomas that are difficult to detect with US [16].

With MRI, all portions of the ALL could be identified in all subjects, including the ligament's origin and insertion. Helito et al. reported a 89.7% detection rate for the femoral portion, a 94.8% detection rate for the meniscal portion, and a 79.4% detection rate for the tibial portion of the ALL by using proton density-weighted MRI sequences. On the other hand, the detection rates were 69.2%, 79.4%, and 64.1% in T2-weighted images, respectively [12]. Although T2-weighted sequences were used in this study, the rate of detection was higher. Helito et al. analyzed coronal, sagittal, and axial views. In contrast, we were able to construct a parallel multiplanar reconstruction of the MRI image of the ALL by using RVS with high quality 3.0-T images and a slice width of 1.0 mm, and were able to confirm the thin fine structure of the ALL.

The femoral and tibial portions were more superficial, and were more easily identified than the meniscal portion by US. In addition, the meniscal portion was thinner than the femoral and tibial portions, and the meniscal portion ran deeper to insert into the lateral meniscus, making it more difficult to identify by US. The femoral origin of the ALL was not identified in 2 cases by the first observer and in 3 cases by the second observer. The femoral origin was close to the popliteal tendon and the LCL, making it more difficult to identify than the tibial insertion. The US measured dimensions of the ALL in this study were

nearly the same as those reported in previous anatomical studies (Table 3). US is superior in space resolving power, and has been reported to be better than MRI in this regard [20]. In addition, US can visualize an area of interest in any limb position, it is not invasive, and it takes less time to perform than MRI. Ongoing improvements in US may allow easier identification of the ALL in the future.

The interobserver reliability of US was statistically significant and similar to that of MRI. Although the ICC of the ALL length was low in US, this was because the length could be measured in only 7 subjects by the first observer and in 6 subjects by the second observer: the femoral origin of the ALL was not identified in 2 cases by the first observer and in 3 cases by the second observer.

The LIGA and ITB were easily identified with US. The ALL runs in the layer between the LIGA and the ITB. Previous anatomical studies and our study revealed that the origin of the ALL is the lateral epicondyle and that the ALL runs across and above the popliteal tendon. In addition, the tibial insertion is < 1 cm from the lateral tibial plateau and approximately halfway between the midpoint of the fibular head and the Gerdy tubercle. By placing the US probe at the lateral epicondyle halfway between the head of the fibula and the Gerdy tubercle, and by making a fine adjustment to depict the tibia cortex of the concave and popliteal fossa, one should be able to identify the ALL.

Using MRI, Claes et al. reported that ALL abnormalities in patients with an ACL injury were situated in the tibial portion in 77.8% of patients and in the femoral portion in 20.4% of patients [11]. In this study, it was not possible to identify the meniscal portion. However, as most ALL injuries occur in the femoral and tibial portions, US may be a useful tool for the diagnosis of ALL injury in these portions. In addition, Doppler US can assess blood flow during the restoration process, and enable a comparison with the contralateral side. US also allows an evaluation of the dynamic motions of the ALL.

There are several limitations of this study. First, the results are limited to the test conditions employed in the study including the use of real-time sonography, evaluation by two experienced orthopedists, and the use of only healthy male subjects. The study results cannot be directly extrapolated to the clinical

setting in patients with acute and chronic ALL injuries. Second, it is not clear whether the same level of diagnostic accuracy can be attained by examiners with less experience in imaging the ALL. Further studies are necessary. Finally, as a small number of subjects were studied in this investigation, additional studies with a larger number of subjects are necessary.

Conclusions

Most portions of the ALL can be identified using US in normal subjects. As most ALL injuries occur at the femoral or tibial portions, US may be useful as a diagnostic tool for ALL injury.

References

1. Segond P. Recherches cliniques et expérimentales sur les épanchements sanguins du genou par entorse. Prog Med 1879;7:297–341.

2. Claes S, Vereecke E, Maes M, Victor J, Verdonk P, Bellemans J. Anatomy of the anterolateral ligament of the knee. J Anat 2013;223(4):321-8.

3. Van der Watt L, Khan M, Rothrauff BB, Ayeni OR, Musahl V, Getgood A, Peterson D. The structure and function of the anterolateral ligament of the knee: a systematic review. Arthroscopy 2015;31(3):569-82.

4. Pomajzl R, Maerz T, Shams C, Guettler J, Bicos J. A review of the anterolateral ligament of the knee: current knowledge regarding its incidence, anatomy, biomechanics, and surgical dissection. Arthroscopy 2015;31(3):583-91.

5. Caterine S, Litchfield R, Johnson M, Chronik B, Getgood A. A cadaveric study of the anterolateral ligament: re-introducing the lateral capsular ligament. [published online ahead of print June 15 2014]. Knee Surg Sports Traumatol Arthrosc 2014. doi:10.1007/s00167-014-3117-z 2014

6. Dodds AL, Halewood C, Gupte CM, Williams A, Amis AA. The anterolateral ligament: Anatomy, length changes and association with the Segond fracture. Bone Joint J 2014;96(3):325–31.

7. Helito CP, Demange MK, Bonadio MB, Tirico LE, Gobbi RG, Pecora JR, Camanho GL. Anatomy and histology of the knee anterolateral ligament. Orthop J Sports Med 2013;1(7):

2325967113513546.

8. Vincent JP, Magnussen RA, Gezmez F, Uguen A, Jacobi M, Weppe F, Al-Saati MF, Lustig S, Demey G, Servien E, Neyret P. The anterolateral ligament of the human knee: an anatomic and histologic study. Knee Surg Sports Traumatol Arthrosc 2012;20(1):147–52.

9. Monaco E, Ferretti A, Labianca L, Maestri B, Speranza A, Kelly MJ, D'Arrigo C. Navigated knee kinematics after cutting of the ACL and its secondary restraint. Knee Surg Sports Traumatol Arthrosc 2012;20(5):870–7.

10. Parsons EM, Gee AO, Spiekerman C, Cavanagh PR. The biomechanical function of the anterolateral ligament of the knee. Am J Sports Med 2015;43(3):669–74.

11. Claes S, Bartholomeeusen S, Bellemans J. High prevalence of anterolateral ligament abnormalities in magnetic resonance images of anterior cruciate ligament-injured knees. Acta Orthop Belg 2014;80(1):45–9.

12. Helito CP, Helito PV, Costa HP, Bordalo-Rodrigues M, Pecora JR, Camanho GL, Demange MK. MRI evaluation of the anterolateral ligament of the knee: assessment in routine 1.5-T scans. Skeletal Radiol 2014;43(10):1421–7.

13. Taneja AK, Miranda FC, Braga CA, Gill CM, Hartmann LG, Santos DC, Rosemberg LA. MRI features of the anterolateral ligament of the knee. Skeletal Radiol 2015;44(3):403–10.

14. Cianca J, John J, Pandit S, Chiou-Tan FY. Musculoskeletal ultrasound imaging of the recently

described anterolateral ligament of the knee. Am J Phys Med Rehabil 2014;93(2):186.

15. Gulsen F, Dikici S, Mihmanli I, Ozbayrak M, Onal B, Obek C, Kantarci F. Detection of bladder cancer recurrence with real-time three-dimensional ultrasonography-based virtual cystoscopy. J Int Med Res 2011;39(6):2264–72.

16. Kitada T, Murakami T, Kuzushita N, Minamitani K, Nakajo K, Osuga K, Miyoshi E, Nakamura H, Kishino B, Tamura S, Hayashi N. Effectiveness of real-time virtual sonography-guided radiofrequency ablation treatment for patients with hepatocellular carcinomas. Hepatol Res 2008;38(6):565–71.

17. Kousaka J, Nakano S, Ando T, Tetsuka R, Fujii K, Yoshida M, Shiomi-Mouri Y, Goto M, Imai Y, Imai T, Fukutomi T, Katsuda E, Ishiguchi T, Arai O. Targeted sonography using an image fusion technique for evaluation of incidentally detected breast lesions on chest CT: a pilot study. [published online ahead of print Nov 6 2014]. Breast Cancer 2014. doi:10.1007/s12282-014-0574-7.

18. Nakano S, Kousaka J, Fujii K, Yorozuya K, Yoshida M, Mouri Y, Akizuki M, Tetsuka R, Ando T, Fukutomi T, Oshima Y, Kimura J, Ishiguchi T, Arai O. Impact of real-time virtual sonography, a coordinated sonography and MRI system that uses an image fusion technique, on the sonographic evaluation of MRI-detected lesions of the breast in second-look sonography. Breast Cancer Res Treat 2012;134(3):1179–88.

19. Sofuni A, Itoi T, Itokawa F, Kurihara T, Ishii K, Tsuji S, Ikeuchi N, Tanaka R, Umeda J, Tonozuka R,

Honjo M, Mukai S, Moriyasu F. Real-time virtual sonography visualization and its clinical application in biliopancreatic disease. World J Gastroenterol 2013;19(42):7419–25.

20. Bearcroft P. Radiology. In: Hutson M, Speed C, editors. Sports injuries. Oxford University Press, Oxford; 2011, p. 129–41.

Nazarian LN. The top 10 reasons musculoskeletal sonography is an important complementary or alternative technique to MRI. AJR Am J Roentgenol. 2008:190(6):1621-6.

Figure captions

Figure 1.

Real-time virtual sonography

US: HI VISION Preirus, Hitachi Aloka Medical, Japan

MRI: Signa EXCITE HDx 3.0T, GE Medical Systems, WI, USA

Figure 2.

The MRI dataset was loaded into the fusion system and displayed together with the ultrasonographic image on the same monitor. Registration was performed in the plane in which the popliteal fossa and the entire lateral collateral ligament (LCL) could be seen at the same time with 30° of knee joint flexion.

MRI: magnetic resonance imaging

Figure 3.

The ligament was divided into three parts: the femoral portion (origin of lateral condyle to the bifurcation point), the meniscal portion (bifurcation to the lateral meniscal insertion), and the tibial portion (bifurcation to the tibial insertion).

Figure 4.

When the ALL was demonstrated in MRI imaging (arrow), the RVS image was frozen and the specifics of the ALL were evaluated in the US images (arrowhead).

ALL: anterolateral ligament, MRI: magnetic resonance imaging, RVS: real-time virtual sonography, US: ultrasonography

Figure 5.

Ultrasonographic view of the ALL (arrowhead)

The proximal portion is to the right and the distal portion is to the left.

LIGA: lateral inferior genicular artery, ALL: Anterolateral ligament

Figure. 1

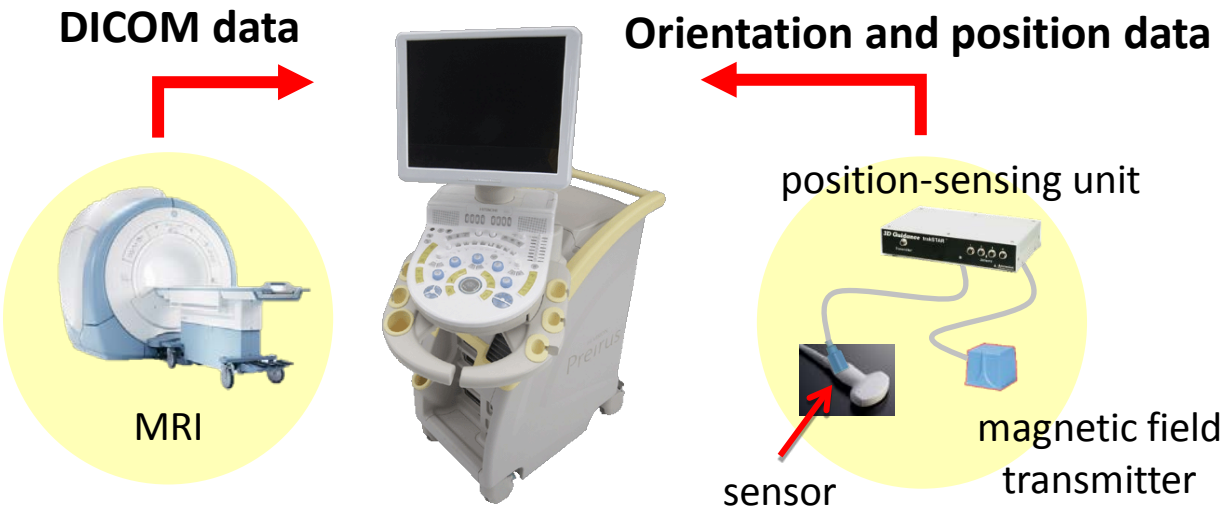
DICOM data
Orientation and position data
position-sensing unit
MRI
magnetic field
transmitter
sensor

Figure. 2

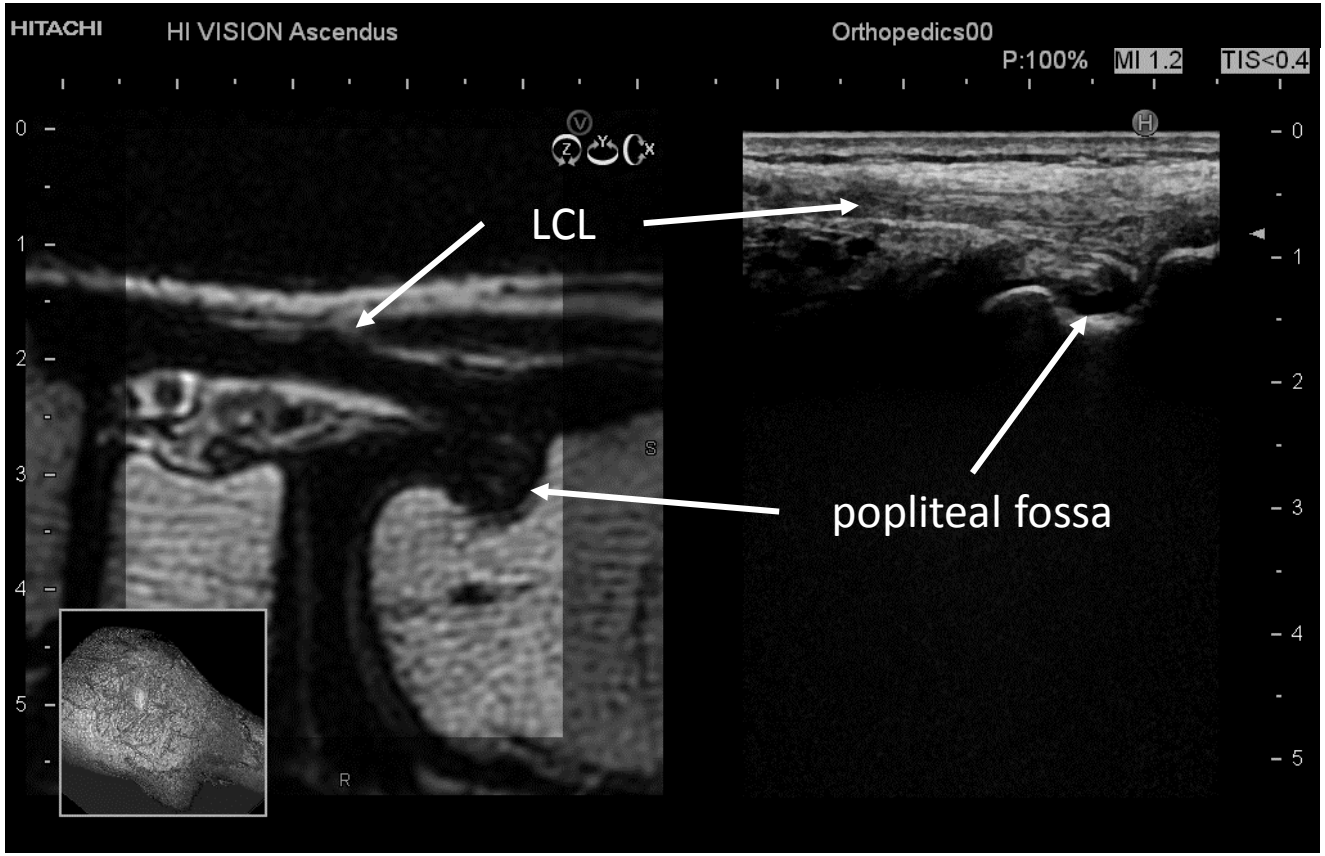
HITACHI
HI VISION Ascendus
Orthopedics00
P:100%
MI 1.2
TIS<0.4
LCL
popliteal fossa

Figure.3

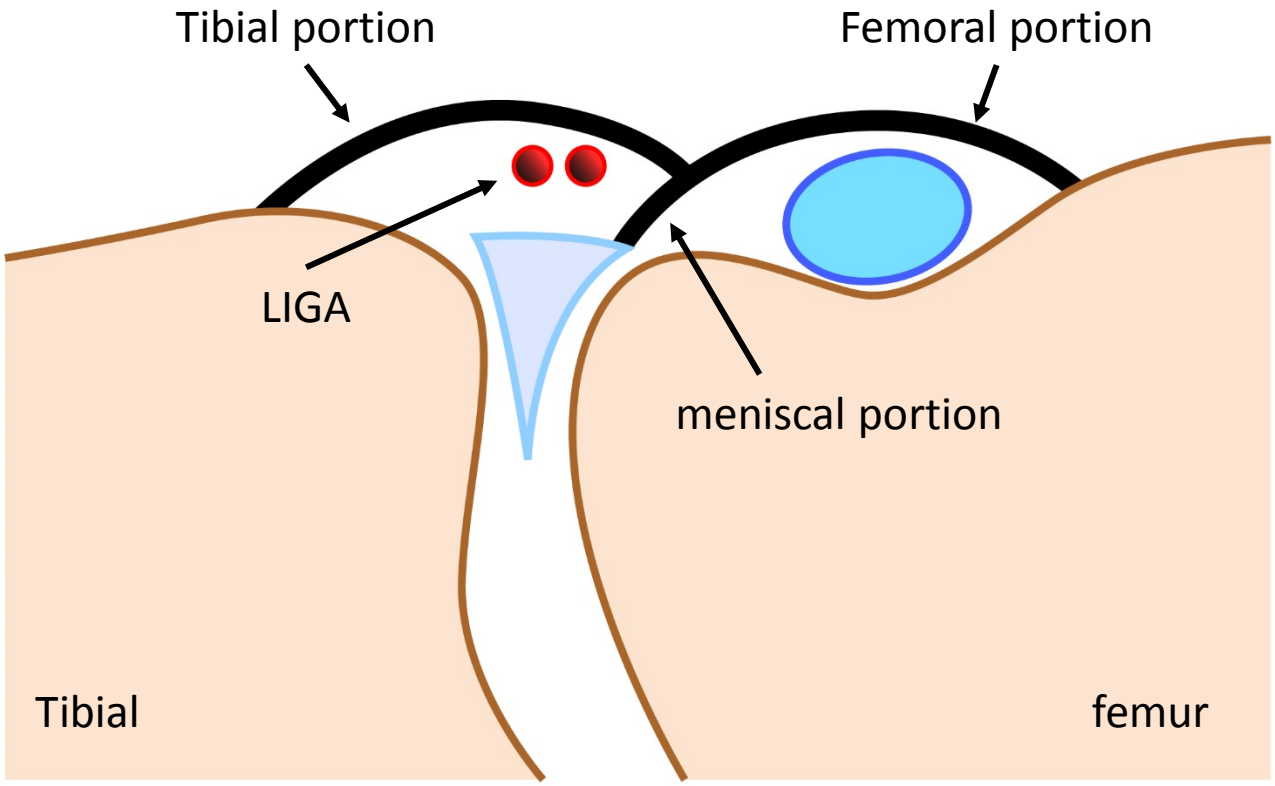
Tibial portion
Femoral portion
LIGA
meniscal portion
Tibial
femur

Figure.4

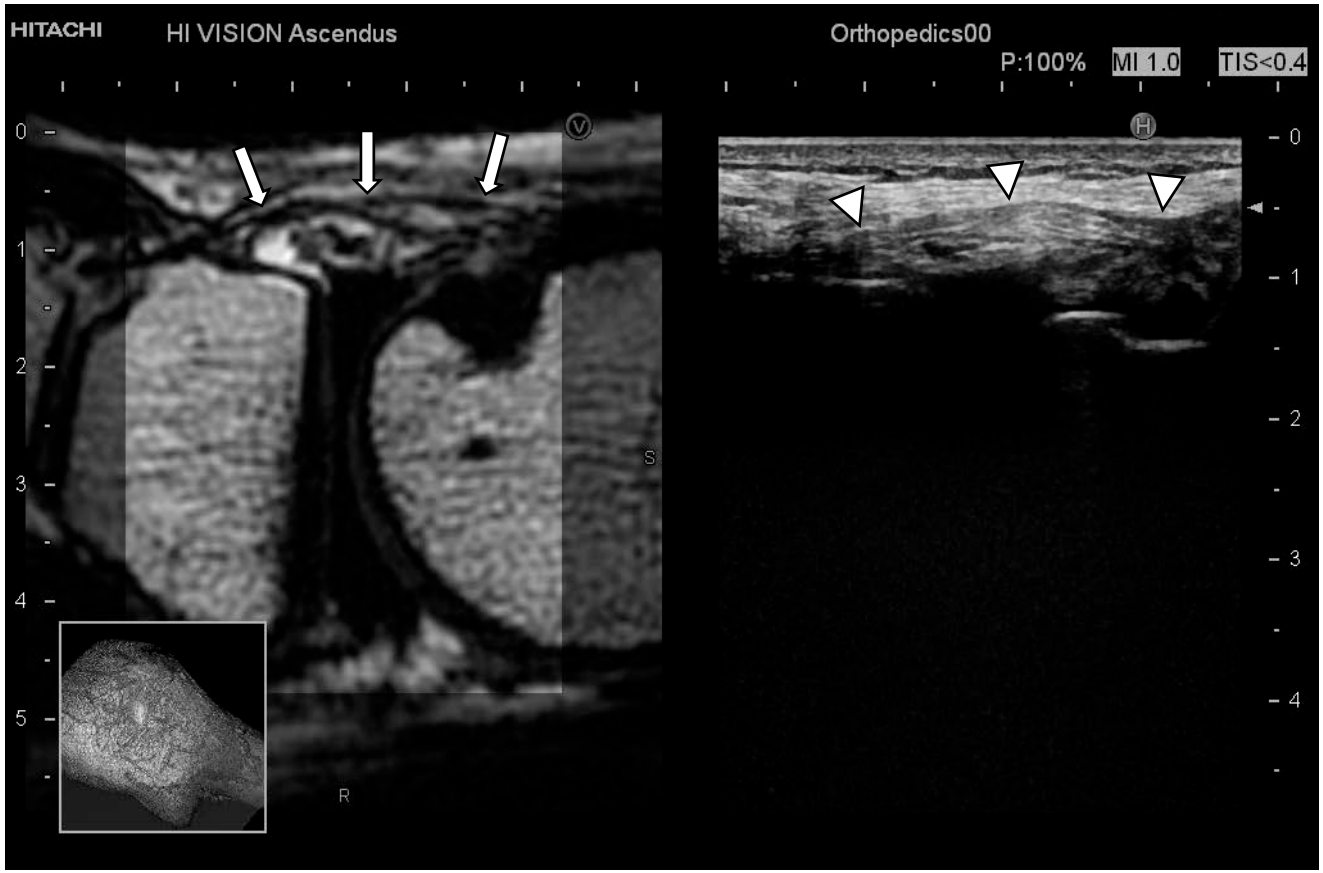
HITACHI
HI VISION Ascendus
Orthopedics00
P:100%
MI 1.0
TIS<0.4
0
1
2
3
4
5
V
H
S
R

Figure.5